Surface-enhanced Raman scattering of silver-gold bimetallic nanostructures with hollow interiors

Yuling Wang, Hongjun Chen, Shaojun Dong, and Erkang Wang

Citation: The Journal of Chemical Physics **125**, 044710 (2006); doi: 10.1063/1.2216694
View online: http://dx.doi.org/10.1063/1.2216694
View Table of Contents: http://scitation.aip.org/content/aip/journal/jcp/125/4?ver=pdfcov
Published by the AIP Publishing

Surface-enhanced Raman scattering of silver-gold bimetallic nanostructures with hollow interiors

Yuling Wang, Hongjun Chen, Shaojun Dong,[a] and Erkang Wang
State Key Laboratory of Electroanalytical Chemistry, Changchun Institute of Applied Chemistry, Chinese Academy of Science, Changchun 130022, Jilin, China and Graduate School of the Chinese Academy of Sciences, Beijing, 100039, People's Republic of China

(Received 13 March 2006; accepted 25 May 2006; published online 27 July 2006)

Surface-enhanced Raman scattering (SERS) activity of silver-gold bimetallic nanostructures (a mean diameter of ~100 nm) with hollow interiors was checked using *p*-aminothiophenol (*p*-ATP) as a probe molecule at both visible light (514.5 nm) and near-infrared (1064 nm) excitation. Evident Raman peaks of *p*-ATP were clearly observed, indicating the enhancement Raman scattering activity of the hollow nanostructure to *p*-ATP. The enhancement factors (EF) at the hollow nanostructures were obtained to be as large as $(0.8\pm0.3)\times10^6$ and $(2.7\pm0.5)\times10^8$ for 7a and 19b (b_2) vibration mode, respectively, which was 30–40 times larger than that at silver nanoparticles with solid interiors at 514.5 nm excitation. EF values were also obtained at 1064 nm excitation for 7a and b_2-type vibration mode, which were estimated to be as large as $(1.0\pm0.3)\times10^6$ and $(0.9\pm0.2)\times10^7$, respectively. The additional EF values by a factor of ~10 for b_2-type band were assumed to be due to the chemical effect. Large electromagnetic EF values were presumed to derive from a strong localized plasmas electromagnetic field existed at the hollow nanostructures. SERS activity of hollow nanostructures with another size (a mean diameter of ~80 nm) was also investigated and large EF for 7a and b_2-type band are obtained to be $(0.6\pm0.3)\times10^6$ and $(1.7\pm0.7)\times10^8$, respectively, at 514.5 nm excitation and $(0.2\pm0.1)\times10^6$ and $(0.6\pm0.2)\times10^7$, respectively, at 1064 nm excitation. Although the optical properties of the hollow nanostructures have not yet been well studied, high SERS activities of the nanostructures with hollow interiors have been exhibited in our report. © *2006 American Institute of Physics*. [DOI: 10.1063/1.2216694]

INTRODUCTION

Since the first discovery of surface-enhanced Raman scattering (SERS) of pyridine on the roughened Ag electrode,[1] a large number of experimental and theoretical researches[2–8] have been done to recognize the nature of the phenomena. In general, there are two separated mechanisms to describe the SERS effect, electromagnetic mechanism[9–11] (EM) and chemical mechanism (CM).[12–14] EM is a long-range effect, which does not require the chemical bond of the molecules to the metal and can be used to explain the enhancement of molecules distant from the metal surface. When the surface has some roughness, under the surface plasmon resonance (SPR), the localized electromagnetic field will be remarkably enhanced. So it is important for SERS that the surface has a certain extent of "surface roughness." CM is a short-range effect, which involves the electronic resonance/charge transfer (CT) between a molecule and a metal surface resulting in an increase in the polarizability of the molecules.

From the originally used metal electrode[15,16] to metal colloid systems,[17–19] the researches about SERS-active substrate have been explored extensively to develop much higher enhancement ability and stability. Silver and gold colloids are most frequently employed metallic systems in SERS. In comparison of silver, gold surface shows a lower surface enhancement factor (EF) in the visible region. So many attempts to obtain silver/gold composite particles have been carried out in order to induce a greater SERS enhancement on gold surface. For example, Freeman *et al.*[20] have studied the SERS properties of Ag-clad Au nanoparticles and proposed that deposition of submonolayers of Ag on preformed colloid Au leads to altered aggregation and SERS enhancement behavior. Rivas *et al.*[21] have studied the SERS activity of mixed silver/gold colloids and investigated the activity of these substrates at different excitation wavelengths. They think that preparation of Ag/Au mixed colloids allows for the combination of the SERS activities of both metals in a broader interval of the electromagnetic spectrum.

Recently, Zhang *et al.* have reported SERS effect of silver colloids with different shapes and concluded the shapes and crystal planes of silver have great effect on SERS enhancement.[22] But all these studies are performed on nanoparticles with solid interiors. In recent years more interests are placed on the synthesis of nanostructures with hollow interiors for their applications in catalysis, drug delivery, and protection of the environment.[23–27] Hollow nanostructures made of metals exhibit surface plasmonic properties and catalytic activity different from that with solid interiors.[28]

[a]Author to whom correspondence should be addressed. FAX: +86-431-5689711. Electronic mail: dongsj@ciac.jl.cn

This kind of special surface plasmonic properties is assumed to be useful in SERS, which have been seldom investigated, especially to bimetallic nanostructures with hollow interiors. In our laboratory, novel silver-gold bimetallic nanostructures with hollow interiors have been synthesized based on colloid seed-engaged replacement reaction and colloid-mediated deposition reactions,[28] which are assumed to have SERS activity because of the special structure. So far, in this work, SERS activity of these silver-gold bimetallic nanostructures with hollow interiors is investigated by assembling them on the silane-modified glass. SERS spectra of *p*-aminothiophenol (*p*-ATP) were obtained on these bimetallic hollow nanostructures at visible (514.5 nm) and near-infrared (1064 nm) excitation. It is widely accepted that the SERS enhancement derives mainly from both EM and CM theories. Herein, the SERS enhancement in our system may also be a combination of EM and CM effect. The contributions of CM and EM to the SERS signal are compared via EF values.

EXPERIMENTAL SECTION

Materials

(3-aminopropyl)-trimethoxysilane (APTMS), HCl, HNO_3, $HAuCl_4 \cdot 3H_2O$, *p*-ATP, trisodium citrate, hydroxylamine hydrochloride, and $AgNO_3$ were all obtained from Aldrich and used without further purification. Milli-Q grade water (>18 MΩ) was used for all solution preparation and experiments.

Preparation of silver-gold bimetallic nanostructures with hollow interiors and active SERS substrate

Silver-gold bimetallic nanostructures with hollow interiors were synthesized by colloid-engaged replacement reaction and colloid-mediated deposition reaction previously reported.[28,29] Briefly, silver nanoparticles were prepared by sodium citrate reduction of $AgNO_3$.[29] The silver-gold bimetallic nanostructures with hollow interiors were prepared by quickly adding 0.2 mL of aqueous 1% $HAuCl_4$ and 0.05 mL of aqueous 0.04*M* NH_2OH to the 5 mL diluted as-prepared silver nanoparticles colloid under violent stirring at room temperature for around 30 min. The mean diameter of the nanostructures is about 100 nm including the size of the hollow interiors, which is approximate to be 60±10 nm, and the shell of the nanostructure is Ag–Au bimetallic alloy.[28] Another size (~80 nm) of bimetallic nanostructures with hollow interiors was prepared by decreasing the volume of aqueous 1% $HAuCl_4$ to 0.05 mL. It should be mentioned that the concentration of as-prepared silver colloid is 9.0×10^{-11} mol/L, which is five times higher than that of obtained bimetallic nanostructures colloid solution (1.4×10^{-11} mol/L).

The active SERS substrate was fabricated by depositing the colloids onto the silane modified glass and allowed to dry in the air. The substrate was soaked into $10^{-4}M$ *p*-ATP ethanol solution for around 2 h, followed by vigorous washing with ethanol. After the evaporation of the solvent, SERS spectra were recorded under the ambient conditions.

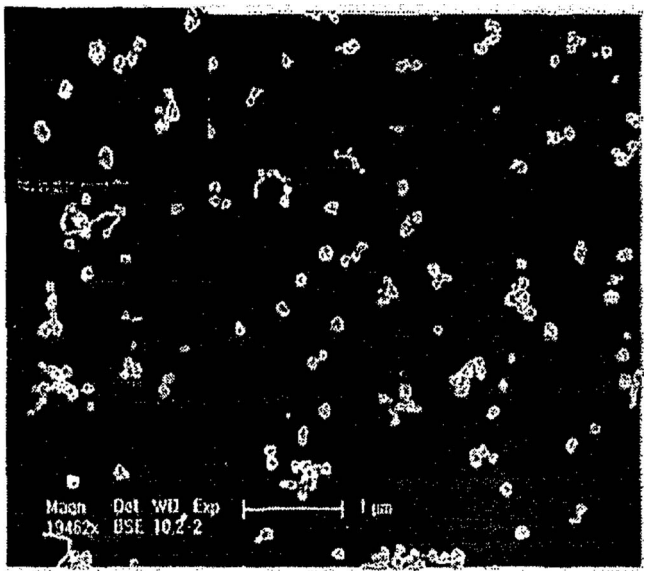

FIG. 1. FE-SEM image of silver-gold bimetallic hollow nanostructures assembled on ITO. Inset shows the high magnification of the SEM image.

Instrumentation

The conductive indium tin oxide (ITO) films with attached silver-gold bimetallic nanostructures with hollow interior and silver nanoparticles were imaged by an XL30 ESEM FEG field emission scanning electron microscopy (FEI Company).

SERS spectra were recorded with a Renishaw system 2000 Raman spectrometer equipped with an integral microscopy (Leica DMLM). Radiation of 514.5 nm was from an Ar^+ ion laser. Raman scattering was collected with a 50× objective (NA=0.75) in 180° configuration and focused into an air-cooled charge-coupled device (CCD) camera. With a holographic grating (1800 g/mm) and a 50 μm slit, a spectral resolution of 1 cm^{-1} can be obtained. A silicon wafer with a Raman band at 520 cm^{-1} was used to calibrate the spectrometer. All of the Raman spectra were recorded in 10 s. All the spectra are base line corrected and noise filtered.

Fourier-transform (FT-)SERS was conducted on Nicrot-960 FT-Raman spectrometer equipped with an InGaAs detector and a Nd/VO_4 laser (1064 nm) as an excitation source. The resolution of the Raman instrument was around 4 cm^{-1} at the excitation wavelength used here and the laser power used was about 300 mW and the scattered light was collected in a 180° geometry. All FT-Raman and FT-SERS were recorded by averaging 256 scans. Additionally, the laser was focused (approximately 100 μm spot size) with a fixed focusing distance for all the samples, which was estimated to be 180 μm.

RESULTS AND DISCUSSIONS

Figure 1 shows field emission scanning electron microscopy (FE-SEM) image of the hollow nanostructures on ITO, in which the hollow interiors of the nanostructures can be clearly observed because the center position was darker than the edge, and the surface coverage of the hollow nanostructures can be obtained to be 3.8 particles/μm^2 from the high

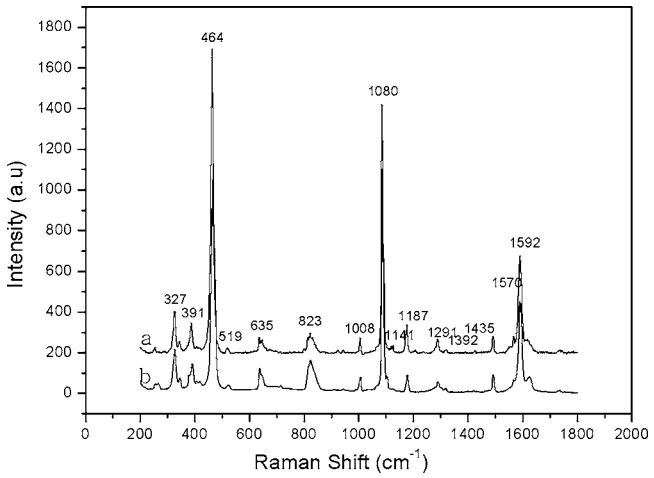

FIG. 2. Raman (a) and FT-Raman (b) spectra of solid *p*-ATP.

magnification of SEM image as shown in the inset of Fig. 1. Meanwhile some aggregates (occupying ~15%) can also be observed, which may be formed at the air-water interface.[30,31]

SERS spectra of *p*-ATP on the silver-gold bimetallic hollow nanostructure with a mean diameter of 100 nm

To investigate the SERS spectra of *p*-ATP on the hollow nanostructures, ordinary Raman (OR) spectra of *p*-ATP are first obtained at 514.5 and 1064 nm as indicated in Fig. 2, which are normal and no difference and to compare the spectra feature, the intensity of FT-Raman spectrum is enlarged 100 times as shown in Fig. 2(b).

Figure 3 shows the SERS and FT-SERS spectra of *p*-ATP on the hollow nanostructures film assembled on the glass at 514.5 and 1064 nm excitation. Distinct Raman peaks of *p*-ATP can be observed clearly at both 514.5 and 1064 nm excitation, indicating the enhancement Raman scattering activity of the bimetallic hollow nanostructures to the *p*-ATP. The spectra features at the two different excitation wavelengths have some differences, which are related to the enhancement mechanisms. The SERS spectrum of *p*-ATP at 514.5 nm excitation is close to that of *p*-ATP adsorbed on the silver film at 514.5 nm reported by Osawa *et al.*[32] and on gold surface at 632.8 nm reported by Cao *et al.*, respectively.[33] Importantly, the SERS spectrum of *p*-ATP at 514.5 nm indicates the shell of the nanostructures is bimetallic because gold has less EM enhancement at 514.5 nm. And this also proves the inference of the reaction mechanism in the synthesis proposed previously.[28] Comparing the OR spectrum of solid *p*-ATP at 514.5 nm as shown in Fig. 2(a), four b_2 modes at 1580, 1435, 1392, and 1141 cm^{-1} and one a_1 mode at 1080 cm^{-1} were largely enhanced on the bimetallic hollow nanostructures. According to the CT theory of Osawa *et al.*, the apparent enhancement of the b_2 modes has been ascribed to the photon-induced charge transfer from the metal to an affinity level of the adsorbed molecule and the four b_2 modes gain their intensity via a Herzberg-Teller contribution.[32]

Notably, FT-SERS spectrum has greatly changed comparing with the SERS spectrum obtained in the visible region. The spectra are dominant with a_1 vibration modes at 1590 and 1078 cm^{-1} and the vibration mode at 390 cm^{-1} is assigned to one of the vibrational modes of the C–S bond, most likely the bending mode of the C–S bond.[34,35] And because a 1064 nm laser was used as the excitation source, a lesser extent of contribution of the Herzberg-Teller term is expected and thereby, the enhancement of b_2 modes is also less than that with the excitation in the visible region.[34,35] The EM mechanism is dominant though the CT mechanism cannot be neglected because of the apparent enhancement of b_2 modes at 1140 cm^{-1}. It has reported that metal nanoshells with shell layers consisting of metals with strong plasmon resonances exhibit a strong, plasmon-derived optical resonance, typically shifted to much longer wavelengths than the plasmon resonance of the corresponding solid metal nanosphere.[28,36] The enhancement at 1064 nm excitation is therefore presumed to mainly derive from electromagnetic mechanism because the SPR of the bimetallic hollow nanostructures is at near-infrared region.[28] It is noteworthy that

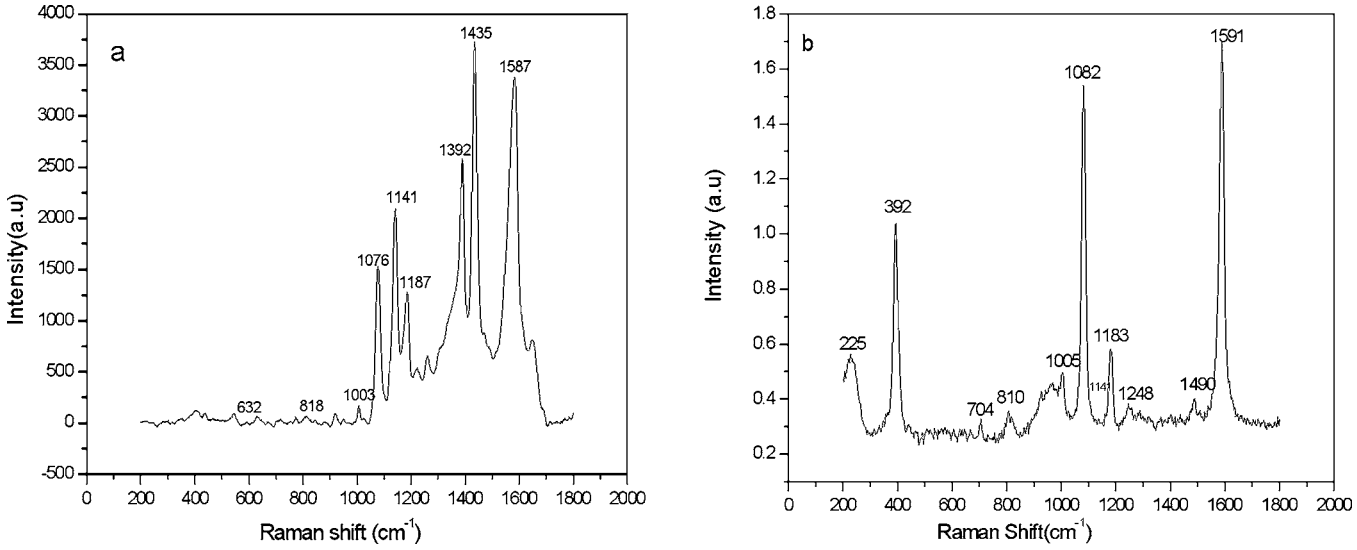

FIG. 3. SERS spectra of *p*-ATP on silver-gold bimetallic hollow nanostructures at 514.5 nm (a) and 1064 nm (b) excitations.

TABLE I. Assignments of ordinary Raman (OR) and SERS spectra of *p*-ATP on silver-gold bimetallic nanostructures with hollow interiors at 514.5 and 1064 nm excitations.

	SERS		
OR	514.5 nm	1064 nm	Assignments[a]
1599(*s*)[b]		1591(*s*)	ν_{CC}, 8*a*(a_1)
1570(*w*)	1587(*s*)		ν_{CC}, 8*b*(b_2)
1435(*w*)	1435(*s*)	1435(*w*)	$\nu_{CC}+\delta_{CH}$, 19b(b_2)
1392(*w*)	1392(*s*)	1392(*w*)	$\delta_{CH}+\nu_{CC}$, 3(b_2)
1187(*m*)	1187(*m*)	1187(*m*)	δ_{CH} 9a(a_1)
1141(*w*)	1141(*s*)	1141(*w*)	δ_{CH}, 9b(b_2)
1080(*m*)	1080(*s*)	1076(*s*)	ν_{CS}, 7a(a_1)
1008(*w*)	1003(*w*)	1005(*w*)	$\gamma_{CC}+\gamma_{CCC}$, 18a(a_1)
823(*w*)	818(*w*)	810(*w*)	π_{CH}, 11(*b*1)
635(*w*)	632(vw)		γ_{CCC}, 12(a_1)
519(*w*)			γ_{CCC}, 16b(b_1)
464(*s*)			γ_{CCC}, 6a(a_1)
391(*m*)		391(*s*)	δ_{CS}
327(*m*)			$\delta_{CH}+\delta_{CS}$, 18b(b_2)

[a]Taken from Refs. 32, 34, 35, 41, and 42. ν stretching; δ, bending; letters in parentheses indicate the vibrational symmetry.
[b]Relative intensities (*s*, strong; *m*, middle; *w*, weak; vw, very weak).

the SERS signal will be far larger at the "hot spot" formed by the aggregated nanostructures than any other places on the glass; our results are typically selected averagely rather than the results produced by hot spot. Assignments of OR and SERS spectra of *p*-ATP on the bimetallic hollow nanostructures are given in Table I, which shows the different spectra features in the visible and near infrared.

The EF values of the hollow nanostructures to *p*-ATP have been estimated by using the following relationship:[37–43]

$$\mathrm{EF} = \frac{I_{\mathrm{SERS}}/N_{\mathrm{ads}}}{I_{\mathrm{bulk}}/N_{\mathrm{bulk}}},$$

where I_{SERS} and I_{bulk} stands for the intensity of a vibrational mode in the SERS and OR spectra of *p*-ATP, respectively. EF values for the 7a and b_2-type mode are determined on the bimetallic hollow nanostructures, and so for all the spectra, the intensity of the ν_{7a} (a_1) at ~1080 cm^{-1} and 19b (b_2) at 1435 cm^{-1} were used to calculate the EF values. N_{ads} and N_{bulk} are the number of *p*-ATP molecules adsorbed on the substrate and bulk molecules illuminated by the laser light to obtain the corresponding SERS and OR spectra, respectively. N_{ads} can be obtained according to the method proposed by Orendorff *et al.*,[39] which is

$$N_{\mathrm{ads}} = N_d A_{\mathrm{laser}} A_N / \sigma,$$

where N_d is the number density of the nanoparticles, A_{laser} the area of the focal spot of laser, A_N is the nanoparticles footprint area, and σ is the surface area occupied by an adsorbed *p*-ATP molecule. According to our previous report,[44] the total number of surface adsorbed molecules within the illuminated laser spot (N_{ads}) can be obtained to be about 1.2×10^5, and the N_{bulk} can be calculated to be about 7.3×10^{10}. Considering the intensity ratio of the ring 7a bands at ~1080 cm^{-1} and b_2-type vibration mode at ~1435 cm^{-1} in Figs. 3(a) and 2(a) was measured to be 1.2 and 433.0, respectively, normalized with respect to the absolute intensity of a silicon wafer (it is necessary to normalize the photon band of a silicon wafer to calibrate the spectrometer to avoid the error from the spectrometer and the wave number position and the intensity of Raman spectrum of the silicon wafer are calibrated to be the same every time), the EF at the bimetallic hollow nanostructures for 7a and b_2 vibrational mode can be calculated to be as large as $(0.8\pm0.3)\times10^6$ and $(2.7\pm0.5)\times10^8$ at 514.5 nm excitation, respectively. It has to be noted that the additional EF values by a factor of 100 for the b_2-type modes may be attributed to the chemical effect, with the remaining contributed by the electromagnetic field,[41,42] which may be derived from the strong localized surface plasmon resonance of hollow nanostructures.

To further illutstrate the SERS activity of the hollow nanostructrues, SERS spectra of *p*-ATP SAM on silver nanoparticles with solid interiors assembed on glass are measured at 514.5 nm excitation, as shown in Fig. 4. Figure 4(a) gives FE-SEM image of silver nanoparticles assembled on glass, which is similar to the literature.[34] The surface coverage of silver nanoparticles (17.6 particles/$\mu\mathrm{m}^2$) on glass is higher than that of silver-gold bimetallic hollow nanostructure, which was induced by the different colloid concentration as methioned in the experiment section. SERS spectrum of *p*-ATP on silver nanoparticles shown in Fig. 5(b) is similar to that on the hollow nanostructures and the EF values on them can be calculated via the similar calculation. Briefly, the N_{ads} is approximated to be 3.4×10^5 and the EF values for 7a and b_2 vibraional mode are calculated to be about $(9.5\pm0.6)\times10^4$ and $3.2\pm0.6\times10^7$, respectively, 7–8 times lower than that on silver-gold nanostructures with hollow interiors. In fact, the EF on each bimetallic hollow nanostructure will be far larger than that obtained on each silver nanoparticle due to their different surface coverage. Herein, the EF values on each one of bimetallic hollow nanostructures and single silver nanoparticle have been determined. Recalling the fact that the EF for 7a and b_2 vibration mode is to be $(0.8\pm0.3)\times10^6$ and $(2.7\pm0.5)\times10^8$, respectively, and that the number of the hollow nanostructures illuminated by laser light was 3.0 particles, the EF values on each one of the hollow nanostructures are estimated to be as large as $(0.3\pm0.1)\times10^5$ and $(9.0\pm0.2)\times10^7$ for 7a and b_2 vibrational mode, respectively, which is 30–40 times larger than that obtained on single silver nanoparticle [$(6.9\pm0.1)\times10^3$ and $(2.3\pm0.1)\times10^6$ for 7a and b_2 vibrational mode, respectively]. As for the composite nanostructures, Chen *et al.* have studied SERS enhancement of Pd–Ag and Pt–Ag nanobox and ascribed the enhancement to the presence of a large proportion of Ag.[45] But in our system, enhancement on the composite nanostructures is better than that of single composite. So the enhancement on the bimetallic hollow nanostructures is assumed not due to the contribution of the presence of

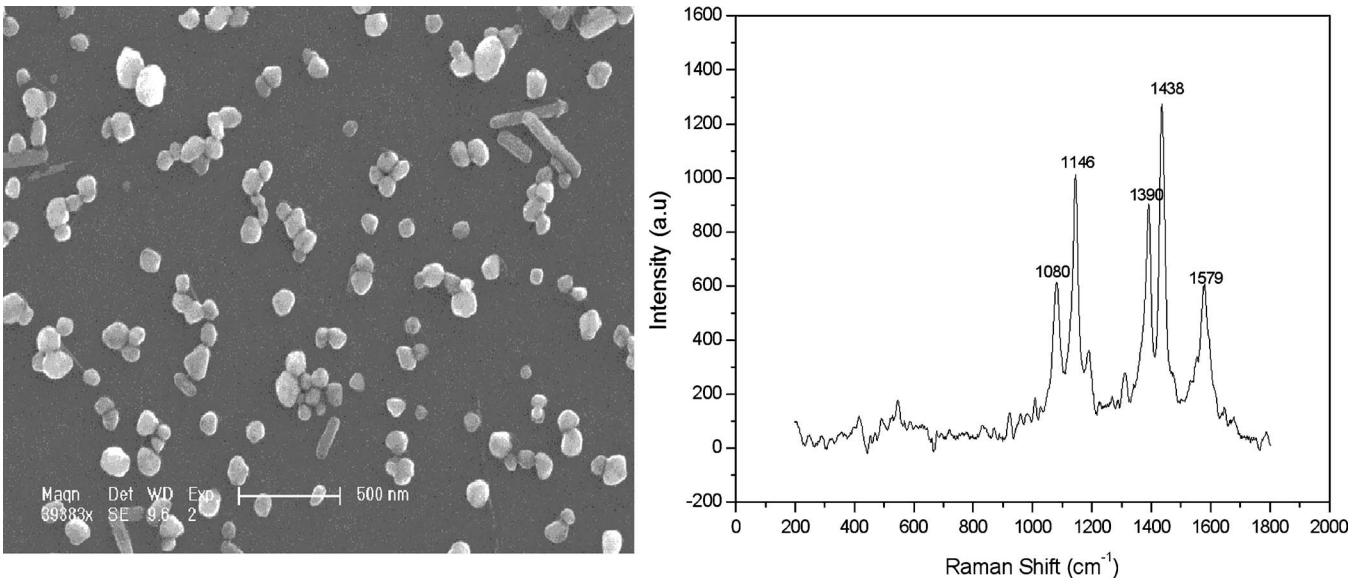

FIG. 4. FE-SEM image of silver nanoparticles assembled on ITO (left) and SERS spectrum of *p*-ATP on silver nanoparticles on ITO (right).

silver but to the surface plasmonic properties produced by the hollow structures. Therefore, high SERS activities of the nanostructures with hollow interiors have been exhibited in our report though the optical properties of the hollow nanostructures have not yet been well studied.

To clearly investigate the derivation of the SERS on bimetallic hollow nanostructures, the EF values were also determined at 1064 nm excitation with a similar calculation. Large EF values are obtained to be $(1.0\pm0.3)\times10^6$ and $(0.9\pm0.2)\times10^7$ for 7a and b_2 vibration mode, respectively.[46] The additional EF values by a factor of ~10 for the b_2-type band is presumed to derive from the chemical effect, with the remaining contributed by the electromagnetic effect. The EF values of all the vibration bands obtained at both 514.5 and 1064 nm excitations are listed in Table II. Comparing the EF values obtained at 514.5 with that at 1064 nm excitation, the contribution of electromagnetic effect to the SERS is evident, indicating the EM provided by the strong localized plasmon resonance at the hollow nanostructures is dominant. And because the SPR of the hollow nanostructures is at near-infrared region,[28] the electromagnetic EF values at 1064 nm are larger than that at 514.5 nm, and meanwhile, the EF from the CM at 1064 nm is weaker than that obtained at 514.5 nm excitation, which demonstrates a lesser extent of contribution of the Herzberg-Teller term at 1064 nm.[34,35] It has to be noted that the high values assigned to the EM enhancement are based only on the assumption that the surface propensity rule taken to the extreme explains that bands are missing,

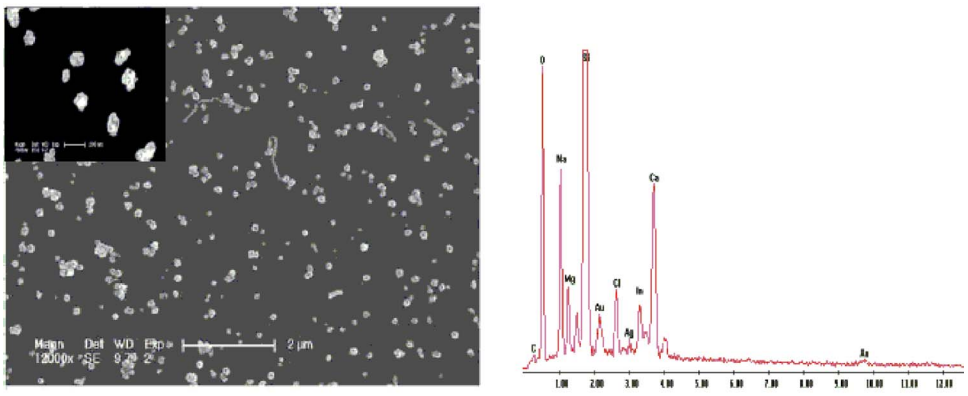

FIG. 5. FE-SEM image (left) and EDX spectrum (right) of silver-gold bimetallic hollow nanostructures assembled on ITO. The bottom table is the parameters from the EDX spectrum and inset shows the high magnification of the SEM image.

Element	Wt %	At %	K-Ratio	Z	A	F
AuM	82.71	72.38	0.8092	0.9865	0.9916	1.0001
AgL	17.29	27.62	0.0903	1.0871	0.4807	1
Total	100	100				

TABLE II. Calculated EF values for all the vibrational bands on silver-gold bimetallic hollow nanostructures with a mean diameter of ~100 nm.

Vibrations	EF values	
	514.5 nm	1064 nm
1592 (ν_{CC},$8a_1$)		$1.1\pm0.3\times10^6$
1570 (ν_{CC},$8b_2$)	$2.4\pm0.5\times10^8$	
1435 ($\nu_{CC}+\delta_{CH}$,$19b_2$)	$2.7\pm0.5\times10^8$	$0.9\pm0.2\times10^7$
1392 ($\delta_{CH}+\nu_{CC}$,$3b_2$)	$1.6\pm0.5\times10^8$	$1.0\pm0.2\times10^7$
1187 (δ_{CH},$9a_1$)	$0.4\pm0.3\times10^6$	$0.2\pm0.3\times10^6$
1141 (δ_{CH},$9b_2$)	$1.4\pm0.5\times10^8$	$0.9\pm0.2\times10^7$
1080 (ν_{CS},$7a_1$)	$0.8\pm0.3\times10^6$	$1.0\pm0.3\times10^6$
1008 ($\gamma_{CC}+\gamma_{CCC}$,$18a_1$)	$0.1\pm0.3\times10^6$	$0.1\pm0.3\times10^6$
823 (π_{CH},$11b_1$)	$0.08\pm0.3\times10^6$	$0.1\pm0.3\times10^6$
635 (γ_{CCC}),$12a_1$	$0.1\pm0.3\times10^6$	
391 (δ_{CS})		$0.7\pm0.3\times10^6$

which can be used to explain the missing and high enhancement of the bands in SERS spectra of *p*-ATP as mentioned above.

SERS spectra of *p*-ATP on another size of bimetallic hollow nanostructures with a mean diameter of 80 nm

To further inquire the SERS activity of silver-gold bimetallic hollow nanostructures and the enhancement mechanism of the hollow nanostructures to *p*-ATP, SERS spectra of *p*-ATP on another size of hollow nanostructures with a mean diameter of ~80 nm have also been investigated.

Figure 5 shows FE-SEM image and energy dispersive x-ray (EDX) spectrum of the bimetallic hollow nanostructures with a mean diameter of ~80 nm. Obviously, the bimetallic hollow nanostructures assembled on the silane modified ITO distribute fairly uniform on the surface and a few aggregates can be observed (occupying ~10% of the total in all), in which the surface coverage of the hollow nanostructures can be obtained to be 4.3 particles/μm^2. EDX spectrum indicates the surface component of the nanostructures are mainly silver and gold and the bottom table in Fig. 5 gives the ratio of silver and gold approximately 1:3, corresponding to the results by x-ray photoelectron spectroscopy (XPS).[28]

TABLE III. Calculated EF for representative vibrations on silver-gold bimetallic hollow nanostructures with a mean diameter of 80 nm.

Excitation wavelength	EF values	
	For 7a at 1080 cm^{-1}	For b_2-type band at 1435 cm^{-1}
514.5 nm	$0.6\pm0.3\times10^6$	$1.7\pm0.7\times10^8$
1064 nm	$0.2\pm0.1\times10^6$	$0.6\pm0.2\times10^7$

SERS and FT-SERS spectra of *p*-ATP on the hollow nanostructures are obtained at 514.5 and 1064 nm excitation as shown in Fig. 6. Obviously, the spectra features of *p*-ATP are similar with that obtained on hollow nanostructures with the diameter of ~100 nm. However, the different enhancement effect on the two sizes of hollow nanostructures can be observed clearly, which was presumed to derive from the different EF values. So the EF values on them are also determined with the similar calculations, which are obtained to be as large as $(0.6\pm0.3)\times10^6$ and $(1.7\pm0.7)\times10^8$ for 7a and b_2-type band at 514.5 nm, and $(0.2\pm0.1)\times10^6$ and $(0.6\pm0.2)\times10^7$ at 1064 nm excitation, indicating the high enhancment Raman scattering activity of hollow nanostrcutures to *p*-ATP. The obtained EF values for the representative vibration bands are listed in Table III.

For these bimetallic hollow nanostructures, chemical effct to EF is estimated to be about 100 in the visible and 10 in the near infrared, which suggests that the difference in enhancment is dependent on electromagnetic effect. A more plausible effect that could explain the differences in EF values between bimetallic nanostrucutures with hollow interiors is the size effect. Maxwell*et al.*[47] have reported the strong relationship between particle size and the excitation wavelength for efficent optical enhancement. In our system, the EF values on bimetallic nanostructures with ~100 nm in

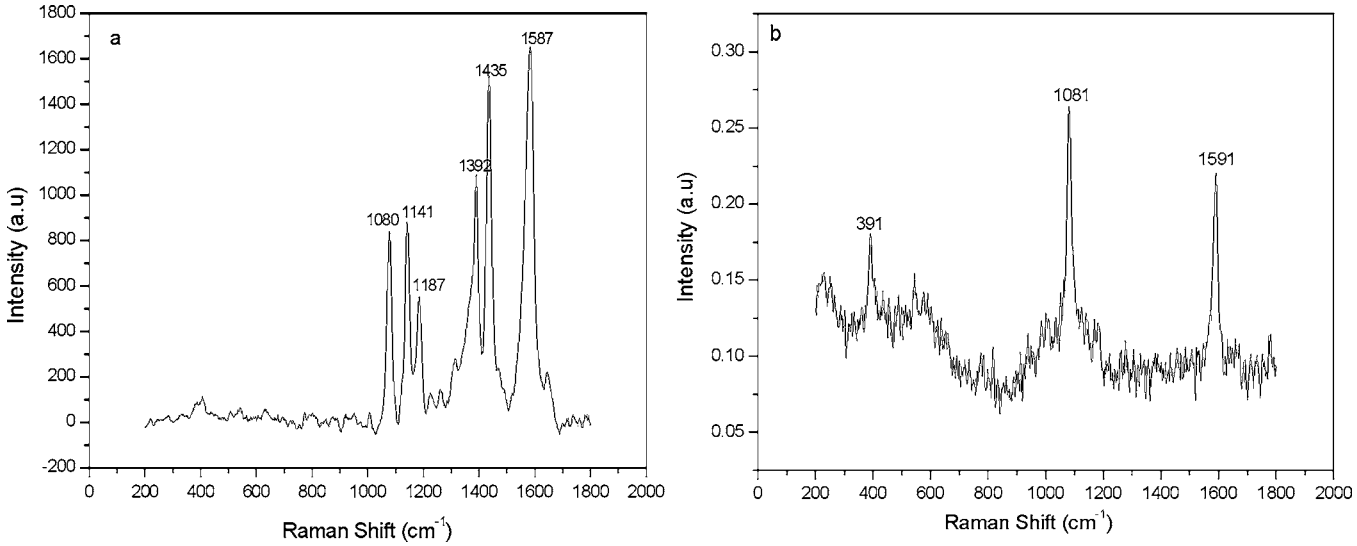

FIG. 6. SERS spectra of *p*-ATP on silver-gold bimetallic hollow nanostructures with a mean diameter of ~80 nm at 514.5 and 1064 nm excitations.

size is larger than that with ~80 nm, which corresponds to the result reported by Maxwell *et al.*[47] As for the core/shell structures, Cao *et al.*[33] have studied the SERS of *p*-ATP on Au (core)/Cu (shell) from theoretical analysis. And meanwhile, Kerker and Blatchford[48] and Baer *et al.*[49] proposed a theory model for SERS on core/shell structure materials. But for core/shell nanostructures with hollow interiors, the electromagnetic coupling may be more complicated and none have been studied. So we expect to work on further experiments to explore the electromagnetic effect between bimetallic hollow nanostructures. Anyway, the large EF values on the hollow nanostructures have clearly indicated the large enhancement Raman scattering activity to the probe molecule, though the optical properties of the hollow nanostructures have not yet been well studied.

CONCLUSION

SERS activity of silver-gold bimetallic nanostructures with hollow interiors has been investigated at 514.5 and 1064 nm excitation choosing *p*-ATP as the probe molecule. Distinct Raman peaks of *p*-ATP on these nanostructures are clearly observed, indicating the enhancement Raman scattering activity of the hollow nanostructures. The EF values for 7a and b_2-type band obtained at 514.5 nm are estimated to be as large as $(0.8\pm0.3)\times10^6$ and $(2.7\pm0.5)\times10^8$, respectively, 30–40 times larger than that on silver nanopariticles with solid interiors. Large EF values are also obtained to be $(1.0\pm0.3)\times10^6$ and $(0.9\pm0.2)\times10^7$, respectively, at 1064 nm excitation, indicating the high SERS activity of the bimetallic hollow nanostructures to the probe molecule. Large EF values are also obtained at another size of bimetallic hollow nanostructures, further demonstrating the high SERS activity of the hollow nanostructures.

ACKNOWLEDGMENT

The work was supported by the National Natural Science Foundation of China (Grant Nos. 20575064 and 20427003).

[1] M. Fleischmann, P. J. Hendra, and A. J. Mcquillan, Chem. Phys. Lett. **26**, 163 (1974).
[2] A. Campion and D. R. Mullins, Chem. Phys. Lett. **94**, 576 (1983).
[3] M. A. Bryant and J. E. Pemberton, Langmuir **6**, 751 (1990).
[4] X. M. Yang, K. Ajito, D. A. Tryk, K. Hashimoto, and A. Fujishima, J. Phys. Chem. **100**, 7393 (1996).
[5] A. Bruckbauer and A. Otto, J. Raman Spectrosc. **29**, 665 (1998).
[6] R. F. Aroca and C. J. L. Constantino, Langmuir **16**, 5425 (2000).
[7] M. Litorja, C. L. Haynes, A. J. Haes, T. R. Jensen, and R. P. Van Duyne, J. Phys. Chem. B **105**, 6907 (2001).
[8] J. Soto, J. D. Fernandez, S. P. Centeno, I. Lopez Tocon, and J. C. Otero, Langmuir **18**, 3100 (2002).
[9] M. Kahl and E. Voges, Phys. Rev. B **61**, 14078 (2000).
[10] V. M. Shalaev and A. K. Sarychev, Phys. Rev. B **57**, 13265 (1998).
[11] M. Moskovits, D. P. Dilella, and K. L. Maynard, Langmuir **4**, 67 (1988).
[12] H. Ueba, Surf. Sci. **131**, 347 (1983).
[13] A. Otto, J. Billmann, J. Eickmans, U. Erturk, and C. Pettenkofer, Surf. Sci. **138**, 319 (1984).
[14] J. F. Arenas, M. S. Woolley, J. C. Otero, and J. I. Marcos, J. Phys. Chem. **100**, 3199 (1996).
[15] F. Ni, H. Feng, L. Gorton, and T. M. Cotton, Langmuir **6**, 66 (1990).
[16] Y. C. Liu and L. Y. Jang, J. Phys. Chem. B **106**, 6748 (2002).
[17] L. Rivas, S. Sanchez Cortes, J. V. Garcia Ramos, and G. Morcillo, Langmuir **17**, 574 (2001).
[18] P. A. Mosier-Boss and S. H. Lieberman, Anal. Chem. **77**, 1031 (2005).
[19] C. McLaughlin, D. Graham, and W. E. Smith, J. Phys. Chem. B **106**, 5408 (2002).
[20] R. G. Freeman, M. B. Hommer, K. C. Grabar, M. A. Jackson, and M. J. Natan, J. Phys. Chem. **100**, 718 (1996).
[21] L. Rivas, S. Sanchez-Cortes, J. V. Garcia-Ramos, and G. Morcillo, Langmuir **16**, 9722 (2000).
[22] J. T. Zhang, X. L. Li, X. M. Sun, and Y. D. Li, J. Phys. Chem. B **109**, 12544 (2005).
[23] F. Caruso, Adv. Mater. (Weinheim, Ger.) **13**, 11 (2001).
[24] K. L. Wooley, Chem.-Eur. J. **3**, 1397 (1997).
[25] H. Huang, E. E. Remsen, T. Kowalewski, and K. L. Wooley, J. Am. Chem. Soc. **121**, 3805 (1999).
[26] D. E. Bergbreiter, Angew. Chem., Int. Ed. **38**, 2870 (1999).
[27] Y. G. Sun, B. Mayers, and Y. N. Xia, Adv. Mater. (Weinheim, Ger.) **15**, 641 (2003).
[28] Y. D. Jin and S. J. Dong, J. Phys. Chem. B **107**, 12902 (2003).
[29] P. C. Lee and D. Meisel, J. Phys. Chem. **86**, 3391 (1982).
[30] J. Hu, B. Zhao, W. Xu, Y. Fan, B. Li, and Y. Ozaki, J. Phys. Chem. B **106**, 6500 (2002).
[31] J. W. Hu, G. B. Han, B. Ren, S. G. Sun, and Z. Q. Tian, Langmuir **20**, 8831 (2004).
[32] M. Osawa, N. Matsuda, K. Yoshi, and I. Uchida, J. Phys. Chem. **98**, 12702 (1994).
[33] L. Y. Cao, P. Diao, L. M. Tong, T. Zhu, and Z. F. Liu, ChemPhysChem **6**, 913 (2005).
[34] J. W. Zheng, X. W. Li, Y. Ji, R. A. Gu, and T. H. Lu, J. Phys. Chem. B **106**, 1019 (2002).
[35] J. W. Zheng, Y. G. Zhou, X. W. Li, Y. Ji, T. H. Lu, and R. A. Gu, Langmuir **19**, 632 (2003).
[36] J. B. Jackson and N. J. Halas, J. Phys. Chem. B **105**, 2743 (2001).
[37] B. Ren, X. F. Lin, Z. L. Yang, G. K. Liu, R. F. Aroca, B. W. Mao, and Z. Q. Tian, J. Am. Chem. Soc. **125**, 9598 (2003).
[38] W. B. Cai, B. Ren, X. Q. Li, C. X. She, F. M. Liu, X. W. Cai, and Z. Q. Tian, Surf. Sci. **406**, 9 (1998).
[39] C. J. Orendorff, A. Gole, T. K. Sau, and C. J. Murphy, Anal. Chem. **77**, 3261 (2005).
[40] A. Otto, I. Mrozek, and C. Pettenkofer, Surf. Sci. **238**, 192 (1990).
[41] K. Kim and J. K. Yoon, J. Phys. Chem. B **109**, 20731 (2005).
[42] K. Kim and H. S. Lee, J. Phys. Chem. B **109**, 18929 (2005).
[43] P. He, H. Liu, Z. Li, Y. Liu, X. Xu, and J. Li, Langmuir **20**, 10260 (2004).
[44] Y. L. Wang, H. J. Chen, S. J. Dong, and E. K. Wang, J. Chem. Phys. **124**, 074709 (2006).
[45] J. Y. Chen, B. Wiley, J. McLellan, Y. J. Xiong, Z. Y. Li, and Y. N. Xia, Nano Lett. **5**, 2058 (2005).
[46] A. Ibrahim, P. B. Oldham, D. L. Stokes, and T. V. Dinh, J. Raman Spectrosc. **27**, 887 (1996).
[47] D. J. Maxwell, S. R. Emory, and S. Nie, Chem. Mater. **13**, 1082 (2001).
[48] M. Kerker and C. G. Blatchford, Phys. Rev. B **26**, 4052 (1982).
[49] R. Baer, D. Neuhauser, and S. Weiss, Nano Lett. **4**, 85 (2004).